JACS
JOURNAL OF THE AMERICAN CHEMICAL SOCIETY
Article
pubs.acs.org/JACS

pH-Triggered, Macromolecule-Sized Poration of Lipid Bilayers by Synthetically Evolved Peptides

Gregory Wiedman,[†,§] Sarah Y. Kim,[‡,§] Elmer Zapata-Mercado,[‡,§] William C. Wimley,[*,∥] and Kalina Hristova[*,†,‡,§]

[†]Department of Materials Science and Engineering, Johns Hopkins University, Baltimore, Maryland 21218, United States
[‡]Graduate Program in Molecular Biophysics, Johns Hopkins University, Baltimore, Maryland 21218, United States
[§]Institute for NanoBioTechnology, Johns Hopkins University, Baltimore, Maryland 21218, United States
[∥]Department of Biochemistry and Molecular Biology, Tulane University School of Medicine, New Orleans, Louisiana 70112, United States

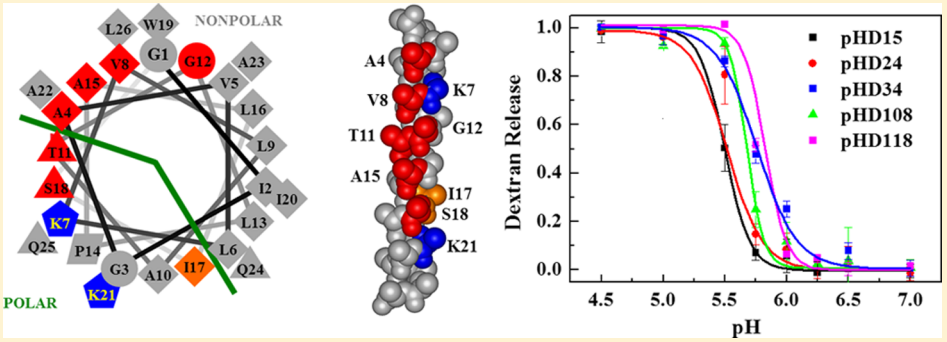

ABSTRACT: pH-triggered membrane-permeabilizing peptides could be exploited in a variety of applications, such as to enable cargo release from endosomes for cellular delivery, or as cancer therapeutics that selectively permeabilize the plasma membranes of malignant cells. Such peptides would be especially useful if they could enable the movement of macromolecules across membranes, a rare property in membrane-permeabilizing peptides. Here we approach this goal by using an orthogonal high-throughput screen of an iterative peptide library to identify peptide sequences that have the following two properties: (i) little synthetic lipid membrane permeabilization at physiological pH 7 at high peptide concentration and (ii) efficient formation of macromolecule-sized defects in synthetic lipid membranes at acidic pH 5 and low peptide concentration. The peptides we selected are remarkably potent macromolecular sized pore-formers at pH 5, while having little or no activity at pH 7, as intended. The action of these peptides likely relies on tight coupling between membrane partitioning, α-helix formation, and electrostatic repulsions between acidic side chains, which collectively drive a sharp pH-triggered transition between inactive and active configurations with apparent pK_a values of 5.5−5.8. This work opens new doors to developing applications that utilize peptides with membrane-permeabilizing activities that are triggered by physiologically relevant decreases in pH.

INTRODUCTION

Membrane-permeabilizing peptides could have utility in a variety of biotechnological and clinical applications due to their ability to breach the barrier imposed by lipid bilayers.[1−10] But to enable their practical application, they will first need to be designed to function only in specific environments, or only in response to specific triggers. One potentially useful trigger is pH, which varies in spatially and temporally specific ways in cellular organelles, and also varies locally in tissues under some pathological conditions, including cancer.[11−13] As an example application, pH-sensitive membrane-permeabilizing peptides could be triggered upon endosomal acidification to promote the release of uptaken polar molecules from endosomal compartments into the cell cytosol.[1,14−16] Such an application would eliminate a long-standing barrier to the delivery of generic polar compounds, especially proteins and other macromolecules, to cells.[14,17,18] Indeed, while efficient methods exist to deliver oligonucleotides to cells,[16,19] most other types of macromolecules are more difficult to deliver. These macromolecules can be directed to existing cellular uptake mechanisms,[20,21] but in the absence of endosome permeabilization or disruption, they often get trapped within the classical pathways that lead to their lysosomal degradation or recycling without significant entry into the cytosol.[22,23] As a second example application, pH-sensitive, membrane-permeabilizing peptides could potentially be used in cancer therapies to selectively permeabilize the plasma membranes of cancer cells. This is possible because the environmental milieu in the vicinity of solid tumors is often acidic due to their high rate of mostly

Received: November 3, 2016
Published: December 21, 2016

DOI: 10.1021/jacs.6b11447
J. Am. Chem. Soc. 2017, 139, 937−945

glycolytic metabolism.[13] In support of this application, the locally acidic pH of solid tumors has already been shown in mice to trigger the pH-sensitive insertion of peptides into membranes, although not for peptides that cause permeabilization.[11,24]

Some progress has been made in the discovery or design of pH-triggered pore-forming peptides,[25,26] including some that we designed rationally,[27] and other pH-triggered membrane-active peptides.[16,28] The state-of-the art in the field has been trial-and-error-based addition of protonatable residues such as aspartate (D), glutamate (E), and histidine (H). Two well-studied examples are pHLIP, which inserts across membranes at pH < 5.5 without permeabilization,[11] and GALA, which permeabilizes synthetic membranes at pH < 5.5.[29] However, none of the known pH-sensitive peptides have all of the properties needed for the applications described above. For example, pHLIP does not form pores, although it can deliver small polar molecules that are covalently attached to it by insertion across the membrane.[30] GALA, and others, do form pores in membranes, but only small pores[28,29,31−33] with limited utility for cellular delivery, especially for macromolecules.

A uniquely useful combination of properties would be pH-triggered membrane permeabilization that enables the movement of macromolecules across membranes. Until recently, even nontriggered macromolecular poration activity that occurs at low peptide concentration has been rare in pore-forming peptides.[34,35] However, we recently used high-throughput screening of a peptide library to discover a unique peptide, called MelP5, which allows macromolecules through synthetic membranes even at very low concentrations of peptide.[36,37] Thus, with MelP5, there is at least one sequence known that is a *non-pH-sensitive* macromolecular pore forming peptide. As discussed above, there are also sequences such as GALA and pHLIP and others that have *pH-sensitive* membrane insertion and permeabilization. However, we are aware of no sequences, other than those discussed below, that have both properties.

There is a lack of detailed molecular understanding of the sequence−structure−function relationships for membrane-active peptides, which hinders their rational design. Here we take a novel high-throughput approach to the discovery of pH-sensitive, macromolecular pore-forming peptides. First, we used the sequence of the macromolecular pore former, MelP5, and sequence features found in GALA and pHLIP to design a rational combinatorial peptide library. We then developed an orthogonal high-throughput screen to identify sequences from the library that have the following two properties in synthetic bilayers: (i) little membrane permeabilization at physiological pH 7 at high peptide concentration and (ii) efficient formation of macromolecule-sized defects in membranes at acidic pH 5 and low peptide concentration. Such peptides will have no effect on membranes at normal cellular pH, but will be triggered by physiologically reasonable acidic pH to form macromolecule-sized pores. We show below that this approach successfully led to the discovery of a conserved motif for pH-triggered, macromolecule sized poration. We expect these unique sequences to ultimately form the basis for multiple applications that utilize changes in pH as a functional trigger.

MATERIALS AND METHODS

Library Synthesis. The peptide library was a one-bead-one-peptide library, synthesized using a split-and-recombine approach described in detail previously.[36,38,39] The library members were synthesized on Tentagel Megabead MB NH_2 resin beads (Rapp Polymere MB300002), coupled to it by a UV-cleavable photo linker, 4-(4-[1-(9-Fluorenylmethyloxycarbonylamino)ethyl]-2-methoxy-5-nitrophenoxy) butanoic acid. After synthesis, side chains were deprotected with a mixture of trifluoroacetic acid and scavengers.[40] Beads were then washed extensively and stored dry at −20 °C prior to use.

To cleave the photolinker and release the library members, beads were first suspended in methanol and dispersed onto a glass plate. The beads were dried thoroughly and then exposed to UV light at 365 nm for 6 h with illumination from plate top and bottom. One day prior to screening, beads were placed into the wells of a 96-well plate, one bead per well. Water and hexafluoroisopropanol (25 μL each) were added to each well, and the plates were exposed to 365 nm UV light for an additional 3.5 h, releasing and extracting the peptide while also evaporating the solvent. Finally, 25 μL of water was added to each well, and the plates were incubated overnight for peptide solubilization. About 0.5 nmol of peptide was extracted from each bead, as quantified by tryptophan fluorescence.

Vesicle Preparation. Large unilamellar vesicles for leakage assays were prepared as previously described[41] in 100 mM potassium chloride, with 10 mM sodium phosphate or 10 mM sodium acetate buffer. For small-molecule leakage, the lipid 1-palmitoyl-2-oleoyl-*sn*-3-glycerophosphocholine (POPC) dried from chloroform, was resuspended in buffer containing: 12.5 mM ANTS, 45 mM DPX, 5 mM HEPES, and 20 mM sodium chloride. For macromolecular leakage assays, lipids were resuspended in buffer with 1 mg/mL TAMRA-biotin-dextran (TBD). Lipid suspensions were frozen and thawed 10 times and then extruded 10 times using a 0.1 um pore size Nuclepore polycarbonate filter.[42] After extrusion, external ANTS and DPX were removed by gel filtration with Sephadex G100. External TBD was removed using streptavidin agarose resin.

Small-Molecule Leakage Assay. Lipid vesicles with entrapped ANTS and DPX were diluted into wells of a 96-well plate containing peptide. After 60 min, vesicle permeabilization was measured by an increase in ANTS fluorescence, with excitation at 350 nm and emission at 519 nm. Fractional leakage was quantified using eq 1:

$$\text{fraction ANTS leakage} = \frac{I - I_{\text{background}}}{I_{\text{Triton}} - I_{\text{background}}} \quad (1)$$

Here I is the intensity at 60 min, $I_{\text{background}}$ is the intensity of a control with vesicles only, and I_{Triton} is the intensity in the presence of vesicles and 0.4% v/v of the detergent Triton X-100, added to solubilize the vesicles and release the ANTS.

Macromolecular Leakage Assay. As described previously,[37] 20 nM Alexafluor488-labeled streptavidin (SA) was added to a solution of vesicles with entrapped TAMRA-biotin-dextran, TBD. This solution was added to wells of a 96-well plate containing peptide, and the plate was incubated for 60 min. Release of the 40 kDa dextran enables TBD-SA complex formation, which leads to quenching of the AF488 fluorescence (excitation 495 nm, emission at 519 nm) by TAMRA. The fraction of macromolecule leakage was determined by eq 2:

$$\text{fraction TBD leakage} = \frac{I_{\text{background}} - I}{I_{\text{background}} - I_{\text{Triton}}} \quad (2)$$

where I is the intensity at 60 min, $I_{\text{background}}$ is the intensity of a vesicle control with no peptide, and I_{Triton} is the intensity in the presence of vesicles and 0.1% v/v of the detergent Triton X-100, added to solubilize the vesicles and release the ANTS.

High-Throughput Screening. In the orthogonal high-throughput screen, we combined the two assays described above and used them in 96-well format as follows.

Step 1. Individual beads were separated into the wells of a plate, and peptides were extracted into a small volume of water as described above. Each bead releases about 0.5 nmol of one peptide sequence from the library.

Step 2. First, 1 mM lipid vesicles in 100 μL of sodium phosphate buffer at pH 7 was added to the peptides in water in the plate from Step 1. These vesicles contained the 350 Da fluorophore ANTS and its

DOI: 10.1021/jacs.6b11447
J. Am. Chem. Soc. 2017, 139, 937−945

Table 1. Sequences of the Peptides Studied Here[a]

Peptide	Sequence	# acidic residues	# helical spacings
Melittin	GIGAVLKVLTTGLPALISWIKRKRQQ	0	0
MelP5	GIGAVLKVLATGLPALISWIKAAQQL	0	0
MelP5_Δ4	GIGAVLKELADGLPALIDWIEAAQQL	4	3
MelP5_Δ6	GIGAVLEELADDLPALIDWIEAAQQL	6	5
pHD Peptides			
pHD15-30	GIGEVLHELADDLPDLQEWIHAAQQL	6	9
pHD24-52	GIGDVLHELAADLPELQEWIHAAQQL	5	6
pHD34-20	GIGEVLKELAADLPELQDWIKAAQQL	5	5
pHD54-73	GIGDVLKELADELPALQEWIHAAQQL	5	5
pHD63-38	GIGEVLKDLAAELPELQEWIHAAQQL	5	6
pHD101-77	GIGEVLKELADELPELQEWIHAAQQL	6	9
pHD108-47	GIGEVLHELAEGLPELQEWIHAAQQL	5	6
pHD118-85	GIGEVLHELADDLPELQSWIKAAQQL	5	7
pHD145-40	GIGDVLKELAEELPLLQEWIKAAQQL	5	5
pHD187-4	GIGEVLKDLADLLPELQEWIHAAQQL	5	7

[a]Top panel: Sequences of the natural bee venom pore-former melittin and its synthetically evolved gain-of-function variant, MelP5,[37] which enables macromolecules to cross bilayers at low P:L. Using patterns from pH-sensitive membrane-active peptides, we previously designed two variants, MelP5_Δ4 and MelP5_Δ6, which exhibit pH-triggered membrane activity but do not induce macromolecular-sized poration.[27] Bottom panel: All of the positive peptides sequenced (see Figure 3). Peptides are named after the plate and well in which the positive bead was identified. For each peptide we list the number of acidic residues, and the number of helical spacings of i to i+3, i to i+4, and i to i+7 between acidic residues.

quencher DPX, entrapped at mM concentrations. After this step, the nominal peptide concentration was 5 μM, and the peptide-to-lipid ratio was roughly 1:200. Leakage, if it occurs, causes an increase in fluorescence of ANTS. A few wells contained controls: vesicles only, 1 nmol of the peptide MelP5 (P:L = 1:100), 4 nmol of MelP5 (P:L = 1:25), or 0.4% v/v of the detergent Triton X-100. The latter two should completely permeabilize the vesicles.

Step 3. After 60 min of incubation, ANTS fluorescence was measured for each well to quantitate small-molecule release using eq 1.

Step 4. Next, to the same wells, a different preparation of vesicles was added. These vesicles have entrapped 40kD TAMRA-biotin-dextran (TBD) and external Alexafluor488 streptavidin. The TBD vesicles were in sodium acetate buffer at pH 4 so that the final pH in each assay well was 5.0. This second addition of vesicles increased the total volume to 200 μL which decreased peptide to 2.5 μM and decreased ANTS vesicle concentration to 0.5 mM. The new TBD vesicles were present at 1.5 mM so that the total peptide to total lipid ratio was roughly about 1:800.

Step 5. After 60 min, the intensity of the AF488-streptavidin was measured to quantitate macromolecule release, which is calculated with eq 2. This orthogonal and sequential screen gives two measurements that are used to identify peptides with the desired properties: (i) small-molecule release at pH 7 and P:L = 1:200, and (ii) macromolecule release at pH 5 and P:L = 1:800.

Circular Dichroism Spectroscopy. Circular dichroism was measured in a JASCO 810 spectropolarimeter. Samples in buffers of various pH were prepared by mixing peptide and vesicle solutions, each prepared at the needed pH. Spectra were collected on samples of 1 mM vesicles and 5 μM peptide in a 1 mm path rectangular quartz cuvette after 1 h of equilibration.

Tryptophan Fluorescence. Membrane partitioning was assessed at various pH values using tryptophan fluorescence in a Fluorolog-3 fluorometer (Jobin Yvon). Peptide and lipid solutions were prepared at individual pH values, and tryptophan fluorescence spectra were measured after 60 min of incubation. Excitation was fixed at 280 nm (slit 5 nm), and emission was collected from 300 to 450 nm (slit 5 nm).

RESULTS

Peptide Library Design. The peptide MelP5 is a highly potent, gain-of-function variant of the cytolytic bee venom peptide melittin that was discovered in a high-throughput screen of a library that used melittin as a template.[36] While the melittin library was screened only for dramatically increased potency of small-molecule release, we later showed that MelP5, the most potent gain-of-function peptide discovered, also releases macromolecules from vesicles at low peptide concentration.[37] Among the many known membrane-permeabilizing peptides, Melp5 is unique in its ability to induce the passage of dextrans up to a molecular weight of 40 000 through bilayers. MelP5 is unstructured in solution, but folds into an amphipathic α-helix in the presence of membranes, into which it inserts, leading to macromolecule-sized membrane disruption at low peptide-to-lipid ratios, P:L $\leq$ 1:500.

Previously, we attempted to rationally design pH sensitive, macromolecular pore-forming peptides[27] by encoding pH-sensing motifs, based on the sequences of the pH-sensitive membrane-active peptides GALA[29] and pHLIP,[11] into the pH-insensitive, macromolecular pore-forming motif in MelP5.[37] The designed peptides, named MelP5_Δ4 and MelP5_Δ6 (see Table 1), had four or six of the residues along the polar face of the putative amphipathic helix changed to glutamate or aspartate to impart pH sensitivity. Placement and spacing of the acidic residues were based on the helical spacings in GALA and pHLIP. We found that these rationally designed peptides gained pH sensitivity, as they permeabilized membranes only at pH < 5.0. But at the same time, they lost the ability to form macromolecular-sized pores,[27] demonstrating that the properties of MelP5, GALA, and pHLIP are only partially additive.

Here, we approached the same goal with combinatorial chemistry and high-throughput screening, instead of rational design. Specifically we designed an iterative 18 432-member library using MelP5 as a template (Figure 1), creating a second-generation library that we screened orthogonally for peptides

DOI: 10.1021/jacs.6b11447
J. Am. Chem. Soc. 2017, 139, 937−945

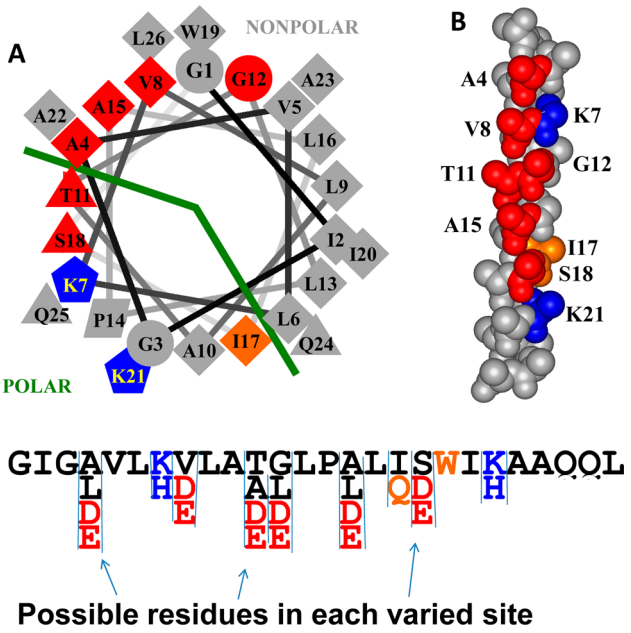

Figure 1. Design of an iterative peptide library. The library is shown in helical wheel and space-filling representations. The library was based on the non pH-sensitive macromolecular pore-former MelP5 which is the sequence shown. Residue shape indicates type in the template sequence of MelP5, with diamonds representing hydrophobic residues and triangles representing polar residues, for example. Colors show residues that were varied in the library. Possible variations present in the library are shown at the bottom. Red positions could be the native residue, or aspartate or glutamate. In some cases, a fourth hydrophobic residue was also possible, as indicated. Blue residues are lysine in MelP5 and could be lysine or histidine in the library members. Position 17 could have the native hydrophobic isoleucine or a polar glutamine. The most important aspect of the library is in the incorporation of six possible protonatable acidic residues, shown in red, that align along one face of the helix, as shown.

that release macromolecules from lipid vesicles at pH 5, but have little or no membrane-permeabilizing activity at pH 7.

In the library, we varied the amino acids at nine positions (Figure 1). Unlike MelP5_Δ4 and MelP5_Δ6, which had a fixed number and pattern of helically spaced acidic residues, the library contained peptides with 0−6 acidic residues distributed in all possible patterns along one face of the MelP5 amphipathic α helix. Our criteria for placement of acidic residues were as follows: (i) maximize the number of i to i+3, i to i+4, and i+ to i+7 α-helical spacings between acidic groups to maximize the electrostatic repulsion between them at neutral pH, and prevent helix formation. For some library members, we expected that such electrostatic repulsion among the acidic side chains will prevent binding and membrane insertion at pH 7 but allow it at pH 5. This pattern also enables library members to form amphipathic helices in which the protonation state of the acidic residues can make a significant contribution to helical propensity and membrane insertion; (ii) retain basic residues at positions 7 and 21 because we hypothesized that changing them to acidic residues in MelP5_Δ4 and MelP5_Δ6[27] may have altered the peptide function; (iii) retain overlap between the polar face of the MelP5 helix and the positions of the new acidic residues; (iv) reduce hydrophobicity as little as possible to maintain the propensity of the helix to partition into membranes; (v) avoid replacing any residues known to be critical to the activity of MelP5, specifically A10, P14, L16, and A23;[36] (vi) avoid replacing tryptophan 19 because it is useful for concentration determination and as an optical probe of structure. With these criteria in mind, we elected to allow both glutamate and aspartate to appear at six positions: A4, V8, T11, G12, A15, and S18, giving the distribution shown in Figure 1. We also allowed the native residue in each of these positions. We allowed hydrophobic leucines to occur at positions A4, G11, and A18 and a somewhat hydrophobic alanine at T11 to modulate hydrophobicity. To potentially compliment the pH sensitivity of the acidic residues, we allowed the native lysines at positions 7 and 21 to also be histidine. Lysine will be cationic at all pH values below 8.5 whereas histidine will be cationic only below its pK_a of ∼6.5.

Previously, we showed that the presence or absence of polar residues at the boundary of the polar−nonpolar faces is a critical feature of MelP5.[36] Specifically, the native T10 in the first generation library was replaced with alanine, which narrows the polar face substantially (Figure 1). In the current library we preserved A10 on the N-terminal half of the peptide and allowed position 17, which defines the cutoff between the polar and nonpolar faces on the C-terminal half of the helix, to vary between hydrophobic isoleucine and polar glutamine.

There are 18 432 unique, 26-residue, MelP5 variants in the library. All library members share at least 17 residues of 26 in common with MelP5 such that the minimum identity is 73%. If we assume that D and E are equivalent, there are 64 different patterns of acidic residues in the library. If D and E are unique, there are 729 different patterns. From the library design in Figure 1, we calculate the following abundance values: 2.8% of library members have six acidic residues (1 pattern of 64), 13.8% have five acidic residues (6 patterns), 28.5% have four acidic residues (14 patterns), 30.6% have three acidic residues (20 patterns), 18.1% have two acidic residues (14 patterns), 5.6% have one acidic residue (6 patterns), and 0.7% have zero acidic residues (1 pattern).

The library was synthesized as a one-bead, one-peptide library using a well-established split-and-recombine approach.[36,38,39] Quality control for the synthesis was done using HPLC, MALDI mass spectrometry, and Edman degradation on peptide extracted from multiple individual beads. These methods showed that every bead examined contained predominantly a single pure sequence and that each sequence observed was, in fact, an expected member of the library. Each 0.3 mm polystyrene solid phase peptide synthesis bead releases about 0.5 nmol of one single sequence as described above.

Orthogonal High-Throughput Screen Results. The library was screened for peptides that simultaneously (i) cause little or no membrane permeabilization at pH 7, even for small-molecule reporters and high peptide concentrations, and (ii) cause macromolecule passage across bilayers at pH 5, at low peptide concentrations. Two different assays, described above, were used in tandem to achieve these aims. One was an assay for release of ANTS, a small molecule (Figure 2A), performed at pH 7. The second was an assay for release of a 40 000 Da TAMRA-biotin-dextran, conducted at pH 5 (Figure 2B). These two assays can be performed in parallel or in series in the same samples because there is no relevant overlap between ANTS fluorescence (ex/em 350/519 nm) and AF488 fluorescence (ex/em 488/505 nm). In the high-throughput screen described in Materials and Methods, the ANTS/DPX assay was conducted at a nominal peptide to lipid ratio of 1:200 at pH 7, and the dextran leakage assay was performed at nominal P:L

DOI: 10.1021/jacs.6b11447
J. Am. Chem. Soc. 2017, 139, 937−945

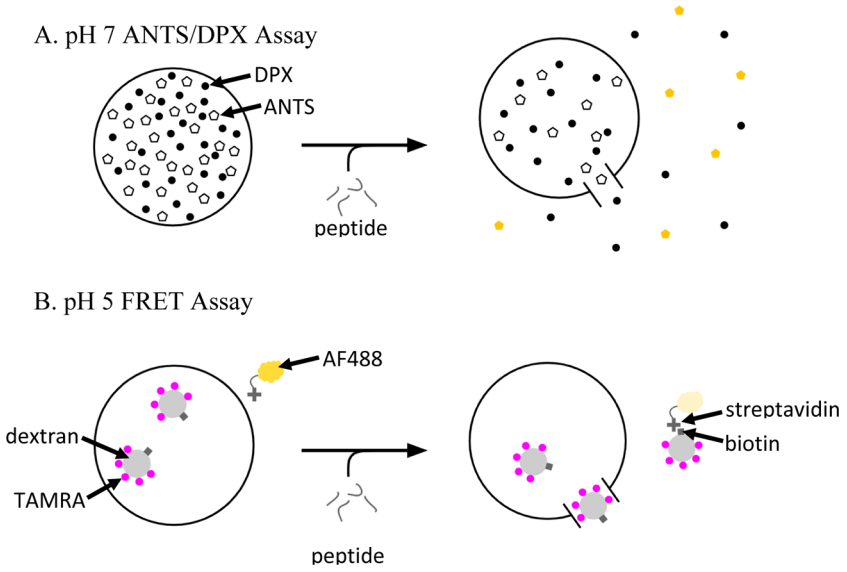

Figure 2. Two different leakage assays are used to measure the pore-forming activity of the peptides and screen for the desired activities. (A) To evaluate leakage of small molecules we co-encapsulate ANTS, a small-molecule dye, and DPX, its obligate quencher, inside lipid vesicles.[52] Membrane destabilization results in release of ANTS and DPX and recovery of ANTS fluorescence. (B) To evaluate leakage of macromolecules, we used a recently published assay[37] based on FRET detection. In this case, a 40 kDa dextran co-labeled with biotin and the acceptor fluorophore, TAMRA, is encapsulated within vesicles. Streptavidin labeled with the donor fluorophore, AlexaFluor488, is on the outside of the vesicles. Upon macromolecular permeation, the TAMRA-biotin-dextran (TDB) can escape and form a complex with streptavidin, allowing FRET to occur. In our high-throughput screen, we measure leakage of ANTS/DPX at pH 7 and nominal P:L = 1:200 and also leakage of TBD at pH 5 and nominal P:L = 1:800.

= 1:800, at pH 5. Because the peptide release from individual beads varies, P:L could vary between individual wells by a factor of 2 or more.

We screened 15 000 library members using the orthogonal high-throughput screen, covering about 80% of the library's sequence space. In Figure 3 we show the ability of each screened peptide to cause small-molecule leakage at pH 7 and macromolecular leakage at pH 5. We present the results in the form of a scatterplot colored according to point density from yellow (highest density) to black (lowest density). Because there were vesicle batch-to-batch variations in the raw intensity values for each assay along the duration of the screen, we have plotted all values in Figure 3 as plate-by-plate *Z*-values; the points plotted are the number of standard deviations from the plate mean, on each axis. The density of points on the *Y*-axis is centered on zero because the distribution of dextran leakage has a symmetrical Gaussian shape. On the other hand, the distribution of points on the *X*-axis is offset from zero because ANTS leakage at pH 7 is asymmetric; many library members cause >80% leakage of ANTS at pH 7.

Four points provide useful landmarks. The activities of 1 nmol and 4 nmol of the template MelP5 under the conditions of the screen are indicated in Figure 3, to compare with 0.5 nmol of each library peptide. We also show values for blank wells with no peptide and for 0.1% v/v Triton X100, which solubilizes all vesicles. A 1 nmol amount of MelP5 causes high small-molecule permeabilization and partial macromolecule release at all pH values. A 4 nmol amount of MelP5 (P:L = 1:100) and 0.1% v/v of Triton X-100 each cause essentially complete release of both types of probes. The activities of most library members are centered on the yellow area in Figure 3; on average they have MelP5-like high leakage of ANTS at pH 7 and moderate leakage of dextran at pH 5. The center of the yellow area corresponds to ∼85% ANTS leakage and ∼30% dextran leakage.

The activity we seek in this work is found in the peptides closest to the upper left corner of Figure 3. These peptides have low small-molecule permeabilization at pH 7 (P:L = 1:200) and high macromolecule permeabilization at pH 5 (P:L = 1:800). Ten library members, shown by red stars in Figure 3, were selected from within this region, and these peptides were sequenced using Edman degradation. Their sequences are shown in Table 1. Below we demonstrate that these selected peptides have exactly the properties we sought in the screen. Thus, our strategy was successful.

Sequence Analysis of Positives. The positive sequences have many features in common with one another, demonstrating that we have identified a family of closely related sequences with a unique, shared activity. *p*-values were calculated against null hypotheses determined by the abundance of the particular residue, class, or motif in the library, using exact binomial statistics. Every positive peptide has five or six acidic residues out of six possible ($p < 10^{-5}$). Positions 4 and 8 are acidic in all positives ($p = 0.002$ and 0.007, respectively). In the remaining four positions that could have acidic groups, 11, 12, 15, and 18, eight of the ten peptides have three acidic residues and one other nonacidic residue and two have six acidic residues. Of the nine possible *i* to *i*+3, *i* to *i*+4, and *i* to *i*+7 helical spacings of acidic groups available, the positive peptides have an average of 6.5 (range 5−9). The constancy of the acidic residue abundance supports the hypothesis, discussed earlier, that pH-triggered membrane activity is determined mostly by the coupling between electrostatic repulsion and the formation of the amphipathic helix as it relates membrane binding (see measurements of helix content below).

Among the 52 selected acidic residues, there was a strong preference for glutamate with 36 glutamates selected compared to 16 aspartates ($p = 0.007$). The preference for E over D is even more striking in the first two and last two possible positions, where 26 of 33 acidic residues were glutamate (p =

DOI: 10.1021/jacs.6b11447
J. Am. Chem. Soc. 2017, 139, 937−945

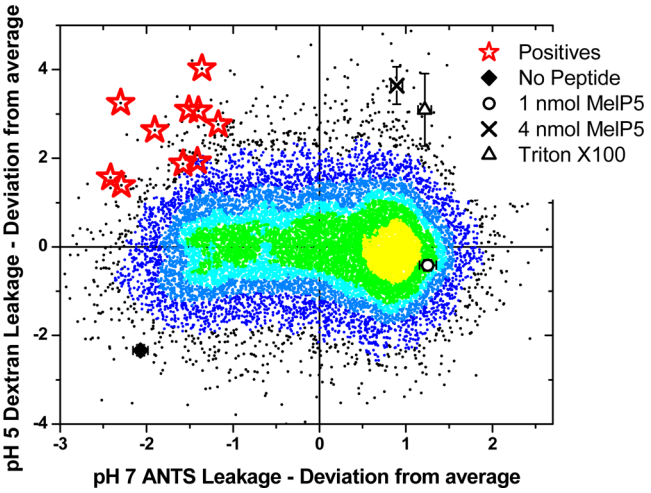

Figure 3. Results of the screen. The serial, two part screen described in Figure 2 was used to assay 15 000 randomly selected library members. Vesicles were made from 100% POPC. The two activities for each of the 15 000 library members are shown as points on a temperature scale, where the point color is determined by point density, from yellow (most dense) to black (least dense). The results of each assay are shown as *Z*-values, or the difference of each point from the plate mean expressed as standard deviations. This approach normalizes for batch-to-batch variations in lipid vesicle intensities in the two assays. About 0.5 nmol of each library member was assayed. For comparison, we also show the values for 1 and 4 nmol MelP5, for Triton-X-100 detergent, which solubilizes vesicles, and for buffer only. The center of the yellow area corresponds to ~85% ANTS leakage and ~30% dextran leakage. Most library members are similar to the template MelP5, but there are outliers in all four quadrants. The peptides we seek, with low ANTS leakage at pH 7 and P:L = 1:200 and high TBD release at pH 5 and P:L = 1:800, are found in the upper left corner. Ten positive sequences, highlighted with red stars, were selected and sequenced using Edman degradation. Their sequences are shown in Table 1.

0.001). We do not currently know why this preference exists, but speculate that the longer side chain of glutamate enables more conformational flexibility of the side chains by which the electrostatic effects can be modulated, either between acidic groups or in the interactions of acidic residues with basic residues. When an acidic residue was possible but not selected, the selected residues included both native residues and the more hydrophobic residues possible, indicating no strong preference for the native residues at positions 11, 12, 15, and 18. Similarly, 9 lysines and 11 histidines were selected in positions 7 and 21, with no obvious preference or pattern. In fact, all possible patterns (KK, HH, HK, and KH) were observed in the 10 positives. We conclude that the identity of the basic side chains and their charge state at pH 7 are of little consequence to the function of these peptides.

Finally, in position 17, where the native, hydrophobic isoleucine and the polar glutamine were possible, we found that the native residue was replaced with glutamine in 10 of 10 peptides (p = 0.002). The current lack of explicit structure−function relationships in these membrane-active peptides makes it difficult to know exactly how this glutamine contributes to activity at this time, but we speculate that its hydrogen bonding capabilities may enable lateral interactions between peptides in the bilayer. We will investigate this and other structural hypotheses in the near future.

It is interesting to compare the positive sequences selected from this library, which have the desired property of macromolecular poration at pH 5.5−5.8, to the rationally designed sequences MelP5_Δ4 and MelP5_Δ6, which have a lower pK_a for permeabilization and do not allow macromolecules across membranes at any pH. The rational and selected peptides both had 4−6 acidic residues with helical spacings. The acidic residues replacing V8, T11, and S18 are present in both families. The rationally designed peptides have 3 or 5 helical spacings between acidic residues, while the selected peptides have 5−9, but there is overlap. In any case, fewer helical spacings should theoretically lead to a higher pK_a whereas the designed peptides actually had a lower pK_a than the selected ones. We replaced one or both basic residues in the designed peptides whereas these positions only contained basic residues in the library because we hypothesized that favorable electrostatic interactions with the basic residues could abrogate acidic repulsions in the library-selected peptides. Furthermore, the designed peptides always had isoleucine in position 17, while the selected peptides always had glutamine at position 17. Isoleucine was available at position 17 in the library, but was never selected. While we can list the differences between our screening successes and our design failures, it is currently not possible to explain or predict these behaviors in molecular terms, effectively demonstrating the power of synthetic molecular evolution. We hope that structural and computational scientists will endeavor to explore these mechanistic questions more deeply in the near future.

Verification of Positive Peptides. Since the selected peptides are very similar to each other, we chose to synthesize and purify a subset of them for detailed validation. Tested peptides included four representative sequences with five acidic residues, pHD24, pHD34, pHD108, and pHD118 as well as pHD15, one of the two with six acidic residues. Because we are interested in pH-triggered macromolecule release at low pH, we validated the positive peptides with both the ANTS assay and the macromolecular release assay using 40 kDa dextran and 53 kDa streptavidin, described above.

Dextran leakage was measured as functions of peptide concentration and pH using vesicles made from phosphatidylcholine lipids. The leakage of 40 kDa dextran from lipid vesicles at P:L = 1:200 as a function of pH is shown for these peptides in Figure 4A. At this concentration, all of the selected peptides cause 100% dextran release at pH 5 and no leakage at pH 7, as desired. Activity occurs only as pH is decreased into the range of pH 6 to 5.5. The apparent pK_a values for the five peptides are similar, ranging from 5.5 to 5.8, with pHD15 having the lowest apparent pK_a value, consistent with it having one more acidic residue. Consistent with this result, and with the screen, we also observe <5% ANTS leakage at at pH 7 (P:L = 1:200) and ~100% leakage at pH 5 (not shown). We note that the macromolecule leakage activity measured in Figure 4 is unique and remarkable, as there are no other peptides known, except for MelP5,[37] that have been shown to release macromolecules from lipid vesicles at such low P:L ratios under any conditions. These synthetically evolved peptides have a pH-triggered version of this activity and release macromolecules at pH 5 even better than MelP5 does at any pH.

Dextran release at pH 5 and pH 7 as functions of peptide concentration (expressed as peptide to lipid ratio, P:L) is shown in Figure 4B, for pHD 15, pHD 24, and pHD 108. The dashed lines show that there is no activity at pH 7, as desired,

DOI: 10.1021/jacs.6b11447
J. Am. Chem. Soc. 2017, 139, 937−945

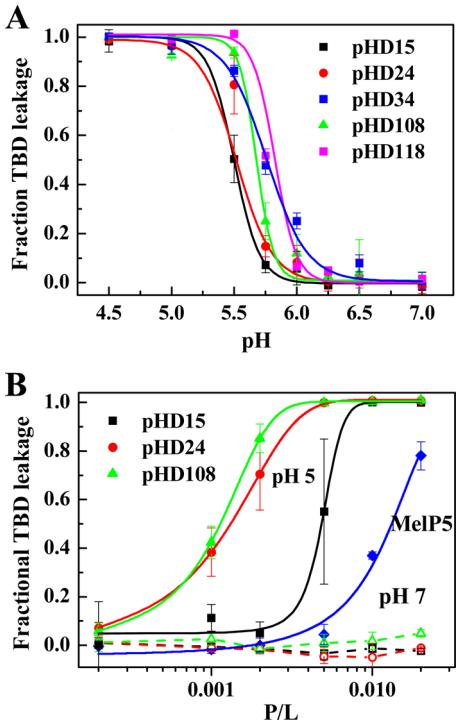

Figure 4. (A) Macromolecule leakage versus pH. A representative set of positive peptides from Table 1 were synthesized and assessed for their ability to promote leakage of a 40 000 Da TAMRA-biotin-dextran (Figure 2B) at P:L = 1:200 and 1 mM POPC vesicles. Changes in pH lead to sharp transition in macromolecular poration. The apparent pK_a values from the curve midpoints range from 5.5 to 5.8. (B) Macromolecule leakage versus concentration. The peptides assessed for their ability to promote leakage of a 40 000 Da TAMRA-biotin-dextran (Figure 2B) at pH 5 and pH 7. The peptides exhibit no activity at pH 7, as desired, even at peptide to lipid ratios as high as 1:50 (dashed lines). At pH 5 all peptides potently cause TBD release with curve midpoints that range from P:L ∼1:900 to 1:600.

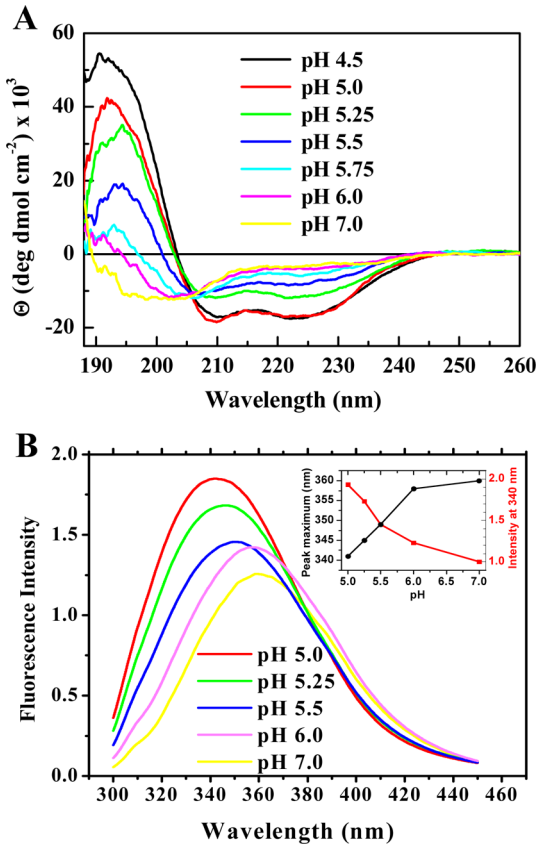

Figure 5. Example binding and folding data. (A) Circular dichroism spectra of pHD108 versus pH at P:L = 1:200 in 1 mM POPC vesicles. Separate samples are made at each pH and equilibrated for 30 min prior to the measurement. The spectra show a structural transition from random coil at pH 7 to classical α-helix at pH 5.75. (B) Tryptophan fluorescence spectra of pHD108 at P:L = 1:200 in 1 mM POPC vesicles. Separate samples are made at each pH and equilibrated for 30 min prior to the measurement. The spectra show a transition from a more polar, water-exposed environment to a less polar, buried environment consistent with peptide that has partitioned into bilayers.

even at peptide to lipid ratios as high as 1:50. However, at pH 5 the selected peptides induce substantial macromolecule leakage with 50% leakage activity at peptide to lipid ratios of 1:900 for pHD108 and 1:750 for pHD24. pHD15, which has six acidic, is the least active of the positives tested, with 50% release at P:L = 1:600. While MelP5 has been shown to release a 10 000 Da dextran at similar concentrations,[37] it releases the 40 000 Da dextran used in this work at ∼ P:L = 1:100. Taken together, these results show that we have successfully identified peptides that are significantly more active than the unique MelP5 and are triggered to act only in acidic pH environments.

We also studied the peptide secondary structure in the presence of vesicles as a function of pH by circular dichroism (CD) spectroscopy. Example CD spectra for pHD108 at P:L = 1:200 (Figure 5A) show a pH-triggered transition from random coil to α-helical structure with an effective pK_a around 5.5. Finally, we measured tryptophan fluorescence as a function of pH at 1:200 which provides a measure of membrane partitioning. Like the CD spectra, example fluorescence spectra for pHD108 (Figure 5B) also show a sharp transition from lower intensity emission at 360 nm to higher intensity and 340 nm emission maximum, consistent with a transition from weak to strong membrane partitioning over the expected pH range of 5−6. In Figure 6 we directly compare the pH dependence of macromolecule leakage, helicity, and tryptophan fluorescence for three peptides at P:L = 1:200, and show that they are very similar, with pK_a of 5.5−5.8, consistent with our hypothesis that leakage, helicity, and binding are coupled for macromolecule release.

DISCUSSION

Several thousand membrane destabilizing peptides, including antimicrobial peptides and other classes of pore-forming peptides, have been described and investigated over the past decades.[35,43−47] Many of these peptides are cationic and destabilize anionic bilayers in a manner driven by strong electrostatic interactions. Efficient permeabilization of zwitterionic phosphatidylcholine (PC) bilayers at low P:L (≤1:100) is uncommon, and efficient release of *macromolecules* from PC vesicles at low P:L ratios was essentially unknown until we reported the discovery of a novel peptide, MelP5.[36] This peptide is unique in its ability to allow the efficient passage of macromolecules through membranes, even at very low peptide-to-lipid ratios (P:L ≤ 1:500 when using 10 000 Da dextran as a probe) where detergent-like vesicle solubilization is unlikely.[33,37] Here, we used MelP5 as a template for an iterative peptide library that we designed and screened to select peptides that cause macromolecular permeabilization of a 40 000 Da dextran at low P:L, like MelP5, but in a pH-dependent manner.

DOI: 10.1021/jacs.6b11447
J. Am. Chem. Soc. 2017, 139, 937−945

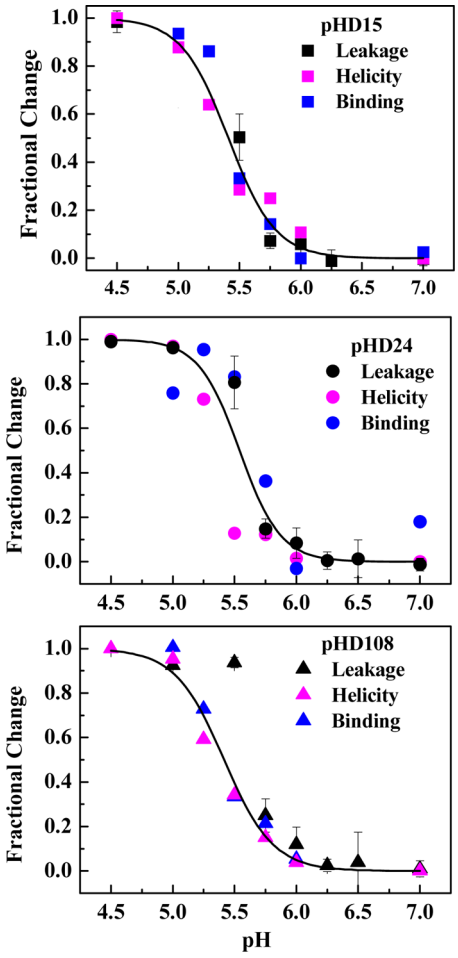

Figure 6. Coupling of binding, structure, and activity. For three pHD peptides we plot changes in TBD leakage, changes in α-helicity from CD, and changes in tryptophan fluorescence as pH is varied. All measurements are at P:L = 1:200. Curves represent the global fit for each peptide of a cooperative transition using all three data sets. There is little or no detectable difference between the pK_a values for leakage, structure, and binding, consistent with our hypothesis that they are coupled.

The peptides that were identified are remarkably potent, macromolecular sized pore-formers at pH 5, while having little or no membrane activity at all at pH 7. Thus, we succeeded in "evolving" MelP5 for gain of function. All of the selected peptides possess exquisite pH sensitivities, with activities transitioning from ~0 to ~100% over one pH unit, centered on apparent pK_a values of 5.5 to 5.8. This success in achieving a goal that we previously failed to achieve using a completely rational design approach[27] highlights the power of synthetic molecular evolution.

Mechanism of Action. All 10 of the positive peptides identified in the library have five or six acidic residues out of the six possible, despite the fact that only 17% of library members have five or six acidic residues. The peptide with six charges that we tested is somewhat less potent and has a lower pK_a than the peptides with five charges (Figure 4B), suggesting that five negative charges arranged with helical spacing on an amphipathic helix are optimal for the observed pH-triggered activity. The fact that we observed various patterns of five acidic residues in the selected positives indicates that the pH sensitivity is due to the physical chemistry of folding and membrane binding. Yet, the specific preference of glutamate compared to aspartate, the overabundance of acidic residues is several positions, and the 100% conservation of glutamine at position 17 suggests that sequence-specific interaction may also play a role in this activity.

According to the Henderson–Hasselbalch equation, an equilibrium that simply reflects protonation of glutamate or aspartate should transition from 10% to 90% complete over two pH units and 1% to 99% over four pH units. However, we observe transitions in dextran leakage, secondary structure and binding by the pHD peptides from near 0% to near 100% over one pH unit (Figure 6), indicative of highly cooperative behavior. Furthermore, the apparent pK_a values that we measure for the selected peptides range from 5.5 to 5.8, much higher than the pK_a of ~3.5 to 4.0 expected for the free side chains for Glu or Asp. We hypothesize that the tight coupling between membrane partitioning, α-helix formation, and electrostatic repulsion between acidic side chains drives both the upward shift in pK_a, relative to that of the free side chains, and the unexpectedly sharp transition. Potentially favorable electrostatic interactions between the basic lysine and histidine residues, and some of the acidic side chains may also contribute to the pH sensitivity.

To estimate the protonation state of the peptide, we used the Membrane Protein Explorer (MPEx)[48] to predict free energies of membrane partitioning of the pHD peptides compared to MelP5. Assuming that bound peptides are 75% α-helix (,[36] Figure 5A), protonation of at least four or five of the acidic side chains in the pHD peptides would be required for strong membrane partitioning that we observed at pH 5. Thus, we hypothesize that most of the acidic side chains in the pHD peptides are cooperatively protonated with an apparent pK_a of 5.5–5.8.

Implications for Peptide Design and Applications. In previous work, we attempted to engineer pH sensitivity into the unique macromolecular poration activity of MelP5, but failed. Here we achieved the goal of pH-triggered macromolecular poration using a fundamentally different approach: synthetic molecular evolution, which is accomplished with orthogonal screening of a rationally designed, iterative, combinatorial peptide library. Despite being able to list similarities and differences between the rationally designed and molecularly evolved peptides, we are not able to identify obvious logical flaws in the rational design approach based on any molecular principle. Specific design principles are not yet apparent from sequence comparison alone. Given the lack of complete understanding of structure–function relations for membrane-active peptides in general, our work shows that synthetic molecular evolution is a powerful, and necessary, method to drive the discovery of novel peptides with specific membrane activities.

The peptides we have selected cause pH-triggered macromolecular poration, a property that could potentially be exploited in multiple ways. For example, there are applications in medicine where acidic environmental pH could be used to trigger the activity of the new peptides. One example is the acidic environment around solid tumors[13] where tumor selective cytolytic activity could be triggered. A second example are acidified organelles, such as endosomes and lysosomes,[17,49−51] where selective cargo delivery into the cytosol could be enabled by pH-induced macromolecular poration. The work described here opens new doors to exploring such

DOI: 10.1021/jacs.6b11447
J. Am. Chem. Soc. 2017, 139, 937–945

applications using peptides with activities that are triggered by a physiologically relevant decrease in pH.

AUTHOR INFORMATION

Corresponding Authors

*wwimley@tulane.edu

*kh@jhu.edu

ORCID

William C. Wimley: 0000-0003-2967-5186

Notes

The authors declare no competing financial interest.

ACKNOWLEDGMENTS

This work was supported by NIH grants GM068619 (K.H.) and GM111824 (W.C.W.). We thank Jing He, Taylor Fuselier, W. Berkeley Kauffman, Charles G. Starr, and Hussain Badani for early brainstorming on the library design.

REFERENCES

(1) Kakudo, T.; Chaki, S.; Futaki, S.; Nakase, I.; Akaji, K.; Kawakami, T.; Maruyama, K.; Kamiya, H.; Harashima, H. *Biochemistry* **2004**, *43*, 5618−5628.

(2) Oliveira, S.; van Rooy, I.; Kranenburg, O.; Storm, G.; Schiffelers, R. M. *Int. J. Pharm.* **2007**, *331*, 211−214.

(3) Kullberg, M.; Owens, J. L.; Mann, K. *J. Drug Target.* **2010**, *18*, 313−320.

(4) Lam, J. K. W.; Liang, W.; Lan, Y.; Chaudhuri, P.; Chow, M. Y. T.; Witt, K.; Kudsiova, L.; Mason, A. J. *J. Controlled Release* **2012**, *158*, 293−303.

(5) Shai, Y.; Oren, Z. *Peptides* **2001**, *22*, 1629−1641.

(6) Kauffman, W. B.; Fuselier, T.; He, J.; Wimley, W. C. *Trends Biochem. Sci.* **2015**, *40*, 749−764.

(7) Komin, A.; Russell, L. M.; Hristova, K. A.; Searson, P. C. *Adv. Drug Deliv. Rev.* **2016**, DOI: 10.1016/j.addr.2016.06.002.

(8) Wimley, W. C.; Hristova, K. *J. Membr. Biol.* **2011**, *239*, 27−34.

(9) Soman, N. R.; Baldwin, S. L.; Hu, G.; Marsh, J. N.; Lanza, G. M.; Heuser, J. E.; Arbeit, J. M.; Wickline, S. A.; Schlesinger, P. H. *J. Clin. Invest.* **2009**, *119*, 2830−2842.

(10) Sani, M. A.; Separovic, F. *Acc. Chem. Res.* **2016**, *49*, 1130−1138.

(11) Andreev, O. A.; Engelman, D. M.; Reshetnyak, Y. K. *Mol. Membr. Biol.* **2010**, *27*, 341−352.

(12) Pantaleo, M. A.; Nannini, M.; Lopci, E.; Castellucci, P.; Maleddu, A.; Lodi, F.; Nanni, C.; Allegri, V.; Astorino, M.; Brandi, G.; Di Battista, M.; Boschi, S.; Fanti, S.; Biasco, G. *Int. J. Oncol.* **2008**, *33*, 443−452.

(13) Gillies, R. J.; Robey, I.; Gatenby, R. A. *J. Nucl. Med.* **2008**, *49* (Suppl 2), 24S−42S.

(14) Duncan, R. *Nat. Rev. Drug Discovery* **2003**, *2*, 347−360.

(15) Heitz, F.; Morris, M. C.; Divita, G. *Br. J. Pharmacol.* **2009**, *157*, 195−206.

(16) Bechinger, B. *Biomol. Concepts* **2012**, *3*, 283−293.

(17) Varkouhi, A. K.; Scholte, M.; Storm, G.; Haisma, H. J. *J. Controlled Release* **2011**, *151*, 220−228.

(18) Raagel, H.; Saalik, P.; Pooga, M. *Biochim. Biophys. Acta, Biomembr.* **2010**, *1798*, 2240−2248.

(19) Majdoul, S.; Seye, A. K.; Kichler, A.; Holic, N.; Galy, A.; Bechinger, B.; Fenard, D. *J. Biol. Chem.* **2016**, *291*, 2161−2169.

(20) Hallbrink, M.; Floren, A.; Elmquist, A.; Pooga, M.; Bartfai, T.; Langel, U. *Biochim. Biophys. Acta, Biomembr.* **2001**, *1515*, 101−109.

(21) Muro, S. *J. Controlled Release* **2012**, *164*, 125−137.

(22) Maiolo, J. R.; Ottinger, E. A.; Ferrer, M. *J. Am. Chem. Soc.* **2004**, *126*, 15376−15377.

(23) Yu, H. J.; Zou, Y. L.; Wang, Y. G.; Huang, X. N.; Huang, G.; Sumer, B. D.; Boothman, D. A.; Gao, J. M. *ACS Nano* **2011**, *5*, 9246−9255.

(24) Yao, L.; Daniels, J.; Wijesinghe, D.; Andreev, O. A.; Reshetnyak, Y. K. *J. Controlled Release* **2013**, *167*, 228−237.

(25) Subbarao, N. K.; Parente, R. A.; Szoka, F. C.; Nadasdi, L.; Pongracz, K. *Biochemistry* **1987**, *26*, 2964−2972.

(26) Parente, R. A.; Nadasdi, L.; Subbarao, N. K.; Szoka, F. C. *Biochemistry* **1990**, *29*, 8713−8719.

(27) Wiedman, G.; Wimley, W. C.; Hristova, K. *Biochim. Biophys. Acta, Biomembr.* **2015**, *1848*, 951−957.

(28) Fendos, J.; Barrera, F. N.; Engelman, D. M. *Biochemistry* **2013**, *52*, 4595−4604.

(29) Parente, R. A.; Nir, S.; Szoka, F. C., Jr. *Biochemistry* **1990**, *29*, 8720−8728.

(30) An, M.; Wijesinghe, D.; Andreev, O. A.; Reshetnyak, Y. K.; Engelman, D. M. *Proc. Natl. Acad. Sci. U. S. A.* **2010**, *107*, 20246−20250.

(31) Nishimura, Y.; Takeda, K.; Ezawa, R.; Ishii, J.; Ogino, C.; Kondo, A. *J. Nanobiotechnol.* **2014**, *12*, 11.

(32) Endoh, T.; Ohtsuki, T. *Adv. Drug Delivery Rev.* **2009**, *61*, 704−709.

(33) Wiedman, G.; Herman, K.; Searson, P.; Wimley, W. C.; Hristova, K. *Biochim. Biophys. Acta, Biomembr.* **2013**, *1828*, 1357−1364.

(34) Mularski, A.; Wilksch, J. J.; Hanssen, E.; Strugnell, R. A.; Separovic, F. *Biochim. Biophys. Acta, Biomembr.* **2016**, *1858*, 1091−1098.

(35) Wimley, W. C. *ACS Chem. Biol.* **2010**, *5*, 905−917.

(36) Krauson, A. J.; He, J.; Wimley, W. C. *J. Am. Chem. Soc.* **2012**, *134*, 12732−12741.

(37) Wiedman, G.; Fuselier, T.; He, J.; Searson, P. C.; Hristova, K.; Wimley, W. C. *J. Am. Chem. Soc.* **2014**, *136*, 4724−4731.

(38) Rathinakumar, R.; Walkenhorst, W. F.; Wimley, W. C. *J. Am. Chem. Soc.* **2009**, *131*, 7609−7617.

(39) Krauson, A. J.; He, J.; Wimley, A. W.; Hoffmann, A. R.; Wimley, W. C. *ACS Chem. Biol.* **2013**, *8*, 823−831.

(40) Atherton, E.; Sheppard, R. C. *Solid phase peptide synthesis*; IRL Press: Oxford, 1989.

(41) Wimley, W. C.; Hristova, K.; Ladokhin, A. S.; Silvestro, L.; Axelsen, P. H.; White, S. H. *J. Mol. Biol.* **1998**, *277*, 1091−1110.

(42) Mayer, L. D.; Hope, M. J.; Cullis, P. R. *Biochim. Biophys. Acta, Biomembr.* **1986**, *858*, 161−168.

(43) Ganz, T.; Selsted, M. E.; Lehrer, R. I. *Eur. J. Haematol.* **1990**, *44*, 1−8.

(44) Lehrer, R. I.; Ganz, T.; Selsted, M. E. *Cell* **1991**, *64*, 229−230.

(45) Brown, K. L.; Hancock, R. E. W. *Curr. Opin. Immunol.* **2006**, *18*, 24−30.

(46) Bechinger, B. *Crit. Rev. Plant Sci.* **2004**, *23*, 271−292.

(47) Dempsey, C. E. *Biochim. Biophys. Acta, Rev. Biomembr.* **1990**, *1031*, 143−161.

(48) Snider, C.; Jayasinghe, S.; Hristova, K.; White, S. H. *Protein Sci.* **2009**, *18*, 2624−2628.

(49) Akinc, A.; Thomas, M.; Klibanov, A. M.; Langer, R. *J. Gene Med.* **2005**, *7*, 657−663.

(50) Erazo-Oliveras, A.; Muthukrishnan, N.; Baker, R.; Wang, T. Y.; Pellois, J. P. *Pharmaceuticals* **2012**, *5*, 1177−1209.

(51) van Dyke, R. W. *Subcell. Biochem.* **1996**, *27*, 331−360.

(52) White, S. H.; Wimley, W. C.; Ladokhin, A. S.; Hristova, K. *Methods Enzymol.* **1998**, *295*, 62−87.

DOI: 10.1021/jacs.6b11447
J. Am. Chem. Soc. 2017, 139, 937−945